We are IntechOpen, the world's leading publisher of Open Access books Built by scientists, for scientists

4,800
Open access books available

122,000
International authors and editors

135M
Downloads

Our authors are among the

154
Countries delivered to

TOP 1%
most cited scientists

12.2%
Contributors from top 500 universities

CLARIVATE ANALYTICS BOOK CITATION INDEX INDEXED

WEB OF SCIENCE™

Selection of our books indexed in the Book Citation Index in Web of Science™ Core Collection (BKCI)

Interested in publishing with us?
Contact book.department@intechopen.com

Numbers displayed above are based on latest data collected.
For more information visit www.intechopen.com

Chapter 1

Analysis of Gas Turbine Blade Vibration Due to Random Excitation

E.A. Ogbonnaya, R. Poku, H.U. Ugwu, K.T. Johnson,
J.C. Orji and N. Samson

Additional information is available at the end of the chapter

http://dx.doi.org/10.5772/58829

1. Introduction

In recent times, a considerable impact has been made on the modeling of dynamic characteristics of rotating structures. Some of the dynamic characteristics of interest are critical speed, systems stability and response to unbalance excitation. In the case of Gas Turbines (GT), the successful operation of the engine depends largely on the structural integrity of its rotor shaft (Surial and Kaushal, 2008).

The structural integrity in turn depends upon the ability to predict the dynamic behavior or characteristic accurately and meet the design requirement to withstand steady and vibratory stresses. An accurate and reliable analysis of the rotor shaft behavior is therefore essential and requires complex and sophisticated modeling of the engine spools rotating at different speeds, static structure like casing, frames and elastic connections simulating bearing (Zhu and Andres, 2007). In this work, GT rotor shaft dynamic modeling will be based on the speed and the force response due to unbalance. During the design stage of GT rotor shaft, the dynamic model is used to ensure that any potential harmful resources are outside the engine operating speed.

Engine vibration tests are part of the more comprehensive engine test program conducted on all development and production engines (Surial and Kaushal, 2008). In the design and retrofit process, it is frequently desirable and often necessary to adjust some system parameters in order to obtain a more favourable design or to meet the new operating requirement Kris, et al (2010). Rotor shaft unbalance is the most common reason in machine vibration (Ogbonnaya 2004).

Most of the rotating machinery problem can be solved by using the rotor balancing misalignment. Mass unbalance in a rotating system often produces excessive synchronous forces that reduce the life span of various mechanical elements (Hariliaran and Srinivasan, 2010). A very small amount of unbalance may cause severe problem in high speed rotating machines. Overhung rotors are used in many engines ring applications like pumps, fans, propellers and turbo machinery. Hence, the need to consider these problems, even at design stages.

The vibration signature of the overhung rotor is totally different from the center hung rotors. The vibration caused by unbalance may destroy critical parts of the machine, such as bearings, seals, gears and couplings. In practice, rotor shaft can never be perfectly balanced because of manufacturing errors, such as porosity in casting, and non-uniform density of materials during operation (Eshleman and Eubanks (2007), Mitchell and Melleu (2005), Lee and Ha (2003)).

1.1. Damped unbalance response analysis

The second part in the rotor shaft dynamic analysis is conducting the damped unbalance response analysis. The objective of this analysis is to accruably determine the critical speeds and the vibration response (amplitude and phase angle) below the trip speed. API 617 (2002) requires that damped unbalance response analysis be conducted for each critical speed within the speed range of 0%-125% of trip speed. The standard requires calculating the amplification factors using the half power method described in figure 1. This helps to determine the required separation margin between the critical speed and the running speed.

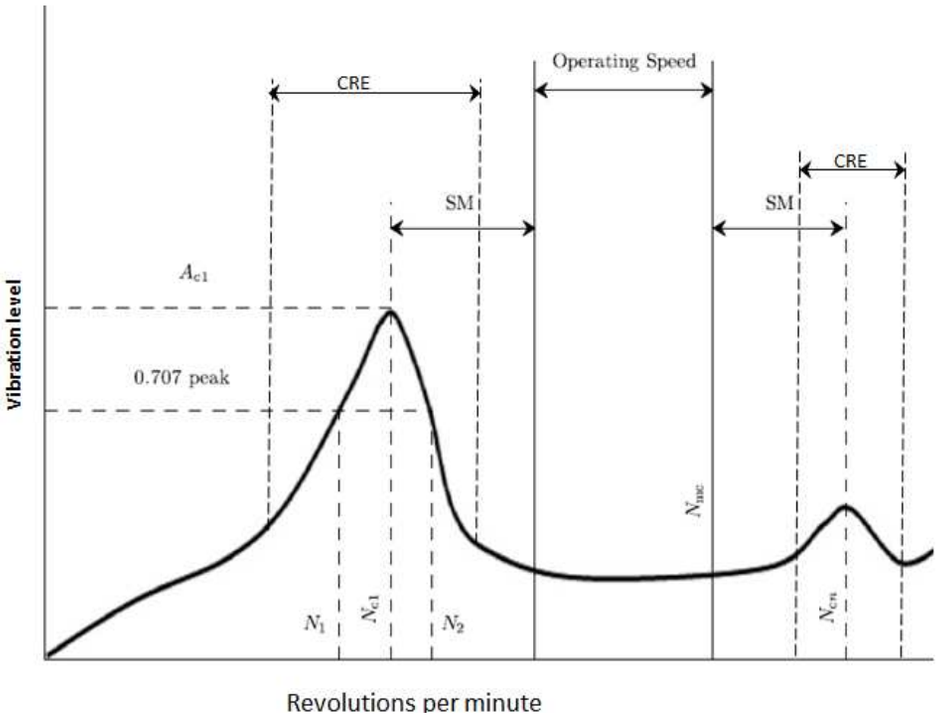

Figure 1. Amplification factor calculation from API 617 (2002)

The Legends in figure 1 are as follows:

N_{C1}=*Rotorfirstcritical,centerfrequency,cyclesperminute*

N_{Cs}=*Criticalspeed,*

N_{mc}=*Maximumcontinuousspeed,105%*

N_1=*Initial(lesser)speedat0.707xpeakamplitude(critical)*

N_2=*Final(greater)speedat0.707xpeakamplitude(critical)*

N_2-N_1=*Peakwidthattheball-powerpoint*

A_f=*Amplificationfactor*

$$= \frac{N_{C1}}{N_2 - N_1}$$

SM=Separationmargin

CRE=Criticalresponseenvelope

A_{c1}=*AmplificationatN*$_{c1}$.

A_{c2}=*AmplificationatN*$_{c2}$

As the amplification factor increases, the required speed increase up to a certain limit. A high amplification factor (AF>10) indicates that the rotor vibration during operation near a critical speed could be considerable and that critical clearance component may rub stationary elements during periods of high vibration.

From the figure 1, a low amplification factor (AF<5) indicates that the system is not sensitive to unbalance when operating in the vicinity of the associated critical speed. To ensure that a high amplification factor will not result in rubbing the standard requires that the predicted major axis peak to peak unbalance response at any speed from zero to trip speed does not exceed 75% of the minimum design diametric running clearances through the compressor.

This calculation is be performed for different bearing clearance and lubricating oil temperatures to determine the effect of the rotor stiffness and damping variation on the rotor shaft response. Also, the standard requires an unbalance response verification test for rotor shaft operating above the critical speeds.

The test results are used to verify the accuracy of the damped unbalance response analysis in terms of the critical speed location and the major axis amplitude of peak response. The actual critical speeds shall not deviate by more than 5% from the predicted, as the actual vibration amplitude shall not be higher than the predicted value (Bader, 2010).

The purpose of this study is therefore to show the dynamic response of a GT rotor shaft using a mathematical model. In the course of this work, it was noted that the rotor shaft can never be perfectly balanced because of manufacture errors. Hence the model involved the following:

a. The working principle of GT rotor shaft

b. Causes of unbalancing on a rotor shaft

c. The response of the system to the critical speed

The objectives and contributions to learning through this work are also as follows:

a. To model the dynamic response of a GT turbine system

b. To consider defects of the rotor shaft on the components of the GT system.

c. The result of this research could thereafter be extended to solve problems on other rotor dynamic engines.

d. To propound a viable proactive integrated and computerized vibration-based maintenance technique that could prevent sudden catastrophic failures in GT engines from rotor shaft.

2. Rotor shaft system and unbalance response

The rotor shaft system of modern rotating machines constitutes a complex dynamic system. The challenging nature of rotor dynamic problem has attracted many scientists, Engineers to investigations that have contributed to the impressive progress in the study of rotating systems.

According to Ogbonnaya (2004), the study of the unbalance responses of GT rotor shaft is of paramount importance in rotor dynamics. He further stated that the GT rotor shaft is a continuous structure and cannot therefore be considered as an idealized lumped parameter beam. Hariliarau and Srinivasan (2010) gave detailed model of rotor shaft coupling. They reviewed the rotor shaft and coupling modeled using Professional Engineer wildfire with the exact dimension as used in experimental setup. A number of analytical methods have been applied to unbalance response such as the transfer matrix method, the finite element method (Lee and Ha, 2003) and the component model synthesis method (Rao, et al 2007; Ogbonnaya, et al 2010).

Unbalance response investigations of geared rotor bearing systems, based on the finite element modeling was carried out by Neriya, et al (2009) and Kahraman, et al (2009) utilizing the model analysis technique. Besides, based on the transfer matrix modeling, Lida et al (2009) and Iwatsubo et al (2009) reported on studies utilizing the usual procedure of solving simultaneous equations while Choi and Mau, (2009) utilized the frequency branching technique to carry out the same analysis.

Further concerning unbalance response investigations of dual shaft rotor-bearing system coupled by bearing, (Hibner, 2007 and Gupta et al., 2003) carried out investigation utilizing the usual procedure of solving simultaneous equations based on transfer matrix modeling. However, all of the above investigations resulted in full numerical solutions of the unbalance response of coupled two shaft rotor bearing systems. On the other hand, Rao (2006) suggested analytical closed-form expressions for the major and minor axis radii of the unbalance response or bit for one-shaft rotor bearing.

2.1. Active balancing and vibration control of rotor system

It is well established that the vibration of rotating machinery can be reduced by introducing passive devices into the system (Gupta, *et al*, 2003). Although an active control system is usually more complicated than a passive vibration control scheme, an active vibration control technique has many age advantages over a passive vibration control technique.

First, active vibration control is more effective than passive vibration control in general (Shiyu, and Jianjun 2001). Second, the passive vibration control is of limited use if several vibration modes are excited. Finally, because the active actuation device can be adjusted according to the vibration characteristics during the operation, the active vibration technique is much more flexible than passive vibration control.

2.1.1. Active balancing techniques

A rough classification of the various balancing methods is shown in figure 2. The most recent development in active balancing is summarized in the dashed-lines shown in figure 2.

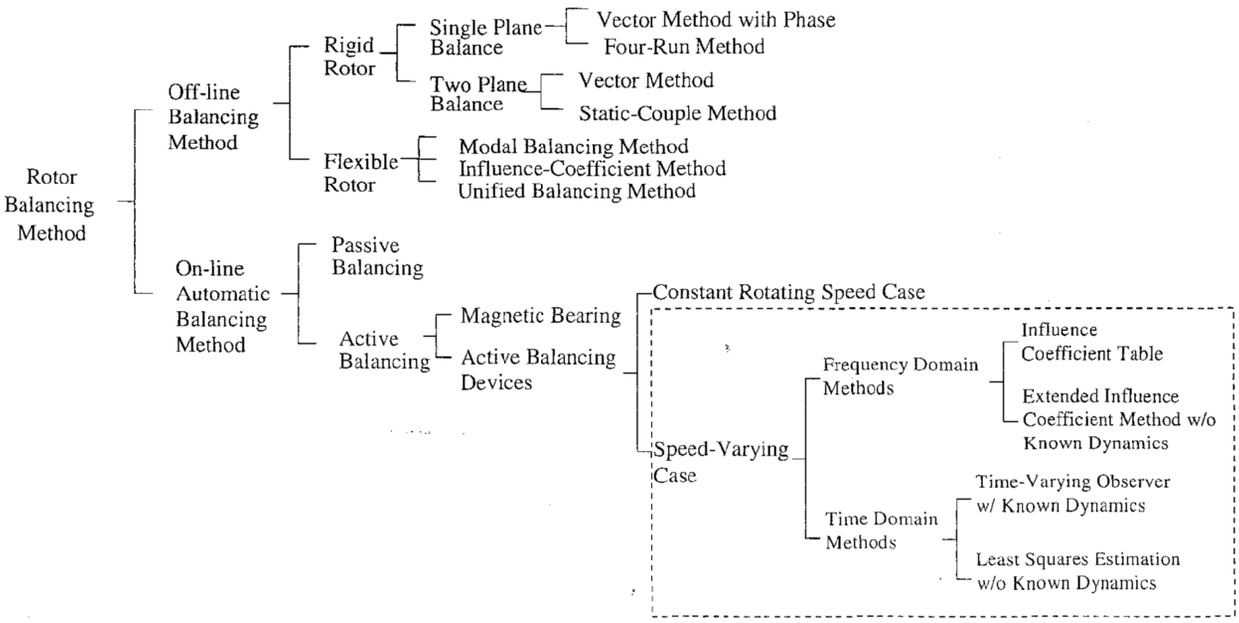

Figure 2. Classification of balancing methods; *Source:ShiyuandJianjun* (2001)

The rotor balancing techniques can be classified as offline balancing methods and real-time active balancing methods. Since active balancing methods are extensions of off-line balancing methods, a review of off-line methods thus is provided (Shiyu and Jianjun, 2001).

2.1.2. Off-line balancing methods

The off-line rigid rotor balancing method is very common in industrial applications. In this method, the rotor is modeled as a rigid shaft that cannot have elastic deformation during operation. Theoretically, any imbalance distribution in a rigid rotor can be balanced in two different planes. Methods for rigid rotors are easy to implement but can only be applied to low-speed rotors, where the rigid rotor assumption is valid. A simple rule of thumb is that rotors operating under 5000 rpm can be considered rigid rotors. It is well known that rigid rotor balancing methods cannot be applied to flexible rotor balancing. Therefore, researchers developed modal balancing and influence coefficient methods to off-line balance flexible rotors.

Modal balancing procedures are characterized by the use of the modal nature of the rotor response. In this method, each mode is balanced with a set of masses specifically selected so as not to disturb previously balanced, lower modes. There are two important assumptions: (1) the damping of the rotor system is so small that it can be neglected and (2) the mode shapes are planar and orthogonal. The first balancing technique similar to modal balancing was proposed by Hibner (2007). This method was refined in both theoretical and practical aspects in Ogbonnaya (2004).

Many other researchers also published works on the modal balancing method, including Rao (2006). Their work resolved many problems with the modal balancing method such as how to balance the rotor system when the resonant mode is not separated enough, how to balance the rotor system with residual bow, how to deal with the residual vibration of higher modes, and how to deal with the gravity sag. An excellent review of this method can be found in Rao (2006). Most applications of modal balancing use analytical procedures for selecting correction masses. Therefore, an accurate dynamic model of the rotor system is required. Generally, it is difficult to extend the modal balancing method to automatic balancing algorithms.

2.2. Self-excitation and stability analysis

The forces acting on a rotor shaft system are usually external to it and independent of the motion. However, there are systems for which the exciting force is a function of the motion parameters of the system, such as displacement, velocity, or acceleration (Ogbonnaya, 2004). Such systems are called self-excited vibrating systems since the motion itself produces the exciting force. The instability of rotating shafts, the flutter of turbine blades, the flow induced vibration of pipes and aerodynamically induced motion of bridges are typical examples of the self-excited vibration (Rao, 2006).

2.3. Dynamic stability analysis

A system is dynamically stable if the motion or displacement coverage or remains steady with time. On the other hand, if the amplitude of displacement increases continuously (diverges) with time, it is said to be dynamically unstable (Ogbonnaya, 2004). The motion diverges and the system becomes unstable if energy is fed into the system through self-excitation. To see the

circumstances that lead to instability, we consider the equation of motion of a single degree of freedom system as shown in equation 1:

$$M\ddot{x} + C\ddot{x} + kx = 0 \tag{1}$$

If solution of the form $x(+)C_e^{st}$ when C is a constant, assuming the equation 1 lead to characteristic equation

$$S^2 + \frac{C}{m}s + \frac{k}{m} = 0 \tag{2}$$

The root of this equation is as shown in equation 3:

$$S_{12} = \frac{C}{2m} + \frac{1}{2}\left[\left(\frac{C}{m}\right)^2 - 4\left(\frac{K}{m}\right)\right]^{1/2} \tag{3}$$

Since the solution is assumed to be $x(+)C_e^{st}$, the motion will be diverging and a periodic, if the roots S_1 and S_2 are complex conjugates with positive real parts. Analyzing the situation, let the roots S_1 and S_2 of equation 2 be expressed as:

$$S_1 = P + iq, \quad S_2 = P + iq \tag{4}$$

Where p and q are real numbers so that:

$$\begin{aligned}\left(S - S_1\right)\left(S - S_2\right) &= S^2 - \left(S_1S - S_2S + S_1S_2\right) = m + \frac{k}{m} \\ &= S^2 + \frac{C}{m}S + \frac{k}{m} = 0\end{aligned} \tag{5}$$

Equations 4 and 5 therefore become

$$\frac{C}{m} = \left(S_1 + S_2\right) = -2P_1\frac{k}{m} = S_1S_2 = P^2 + q^2 \tag{6}$$

From equation (6), it is shown that for negative P_1, c/m must be positive and for positive $P^2 + q^2$, $\frac{k}{m}$, must be positive. Thus the system will be dynamically stable if C and k are positive (assuming that M is positive).

2.3.1. Balancing operation and result

The necessary mass was added at the chosen shaft end shown in figure 3 in order to determine the desired dynamic behaviour. Due to the relatively small rotor radius, it was necessary to use a significant mass; otherwise the obtained influence would have been too low.

Figure 3. Picture of the used balancing plane; *Source:ShiyuandJianjun* (2001)

2.4. Rotor dynamic model of the shaft line

The complete shaft line was modeled (figure 4) by using the MADYN 2000 software. The model was based on scaled drawings. The four fluid film bearings were calculated with the ALP3T program. The static load of the different bearings was determined by aligning the shaft only, taking into account the flexibility of the different rotors, in a way that the couplings are free of bending moments. The present oil film thickness at nominal speed was not considered in this static calculation.

All bearing pedestals were modeled as pure stiffness and mass. This assumption was tested by performing impact tests on the bearing structure in both vertical and horizontal direction. No resonance frequencies were detected below 50Hz or at multiples of this frequency. Therefore it was decided to determine the static stiffness obtained at 50Hz and use this value for the complete frequency range of the different calculations.

There was only poor rotor dynamic information given by the manufacturer, so it was not possible to completely verify the model. However, the calculated results fitted both the basic available rotor dynamic info arid the measured vibration data quite well. From the calculated eigen values at 50Hz two modes seemed to be present near the operating speed of the shaft line (figure 4).

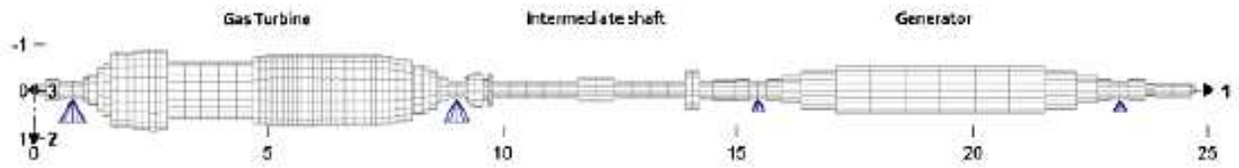

Figure 4. Rotor dynamic shaft line model; *Source: Kris, et. al* (2010)

The closest modes influencing the dynamic behaviour are at respectively 51.9Hz and 53.3Hz. The first eigen mode is the second vertical bending mode of the gas turbine and is unlikely to be causing high vibrations near the generator shaft end. The second eigen mode is a horizontal bending mode of the shaft end. From the eigenvalue analysis it is clear that the damping factor is poor and the mode deformation is almost completely planar (whirling factor of 0). This mode shape is shown in figure 5 and shows clearly the planar deformation near the shaft end. As shown in figure 6, shaft lines can also be represented in 3-D mode shape.

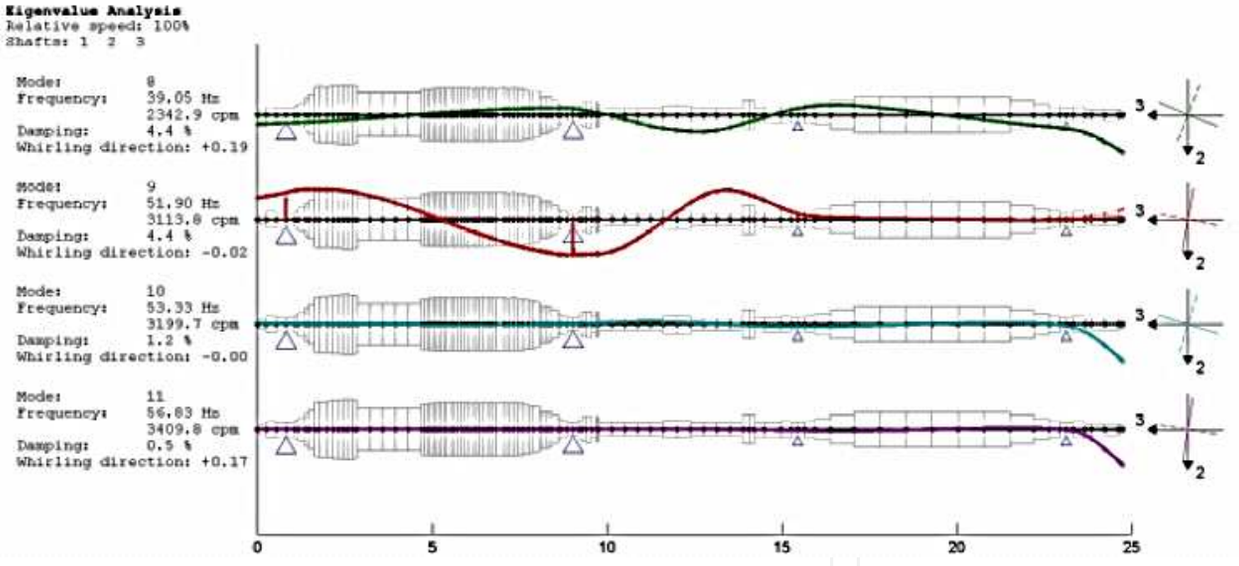

Figure 5. Eigenvalue analysis of the shaft line; *Source: Kris, et. al* (2010)

Based on the measured direct orbit shapes, it was possible to conclude that it was this shaft end mode that was responsible for the high shaft vibrations causing the automatic shutdown of the unit during startup (figure 7). One can clearly see that there is a local horizontal deformation at the generator nondestructive examination measuring plane near nominal speed; but for all the other measuring planes, the relative shaft vibration amplitudes remain rather low.

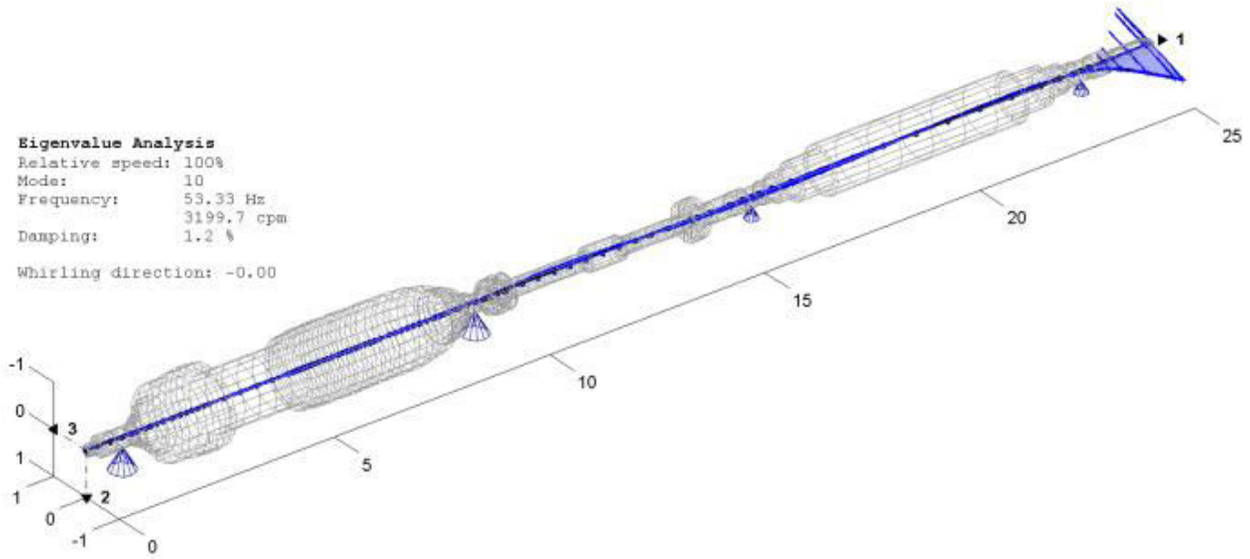

Figure 6. 3D mode shape of the bending critical of the shaft end; *Source: Kris, et. al* (2010)

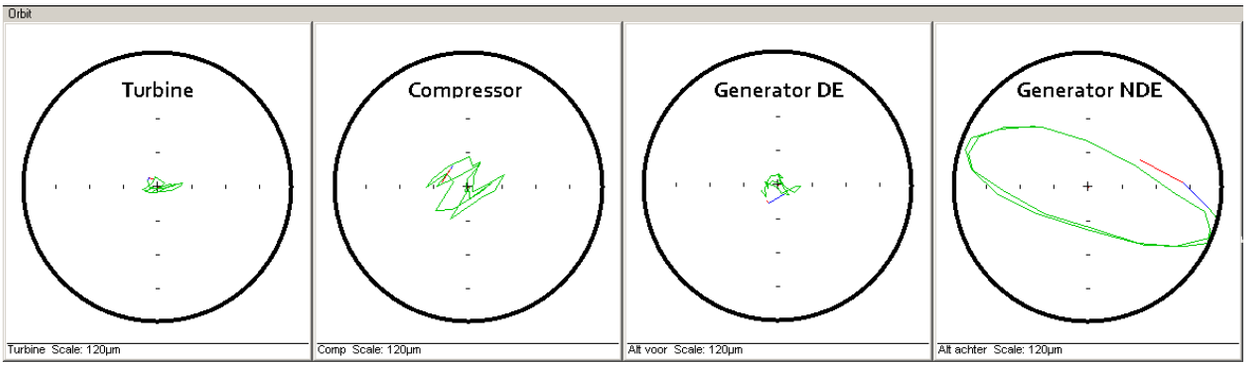

Figure 7. Direct orbit plots at 2980rpm; *Source:Gupta,etal* (2003)

From these results, it was also clear that the "usual" balancing planes at both ends of the generator rotor were not recommended to balance this present unbalance. However, from local inspections of the shaft end, it became clear that it would be possible to do a balancing test run with a mass connected at the end of the shaft line on a rather non-conformistic plane (figure 8). This plane would be the best location because the mode deformation is the highest at the shaft end. This location would also make the balancing plane easily accessible for further adjustment of the mass.

An unbalance calculation was done in order to have an idea of the expected response of the generator. The used weight for this calculation was determined by applying a GT unbalance; based on the weight of this free shaft end (figure 9).

http://dx.doi.org/10.5772/58829

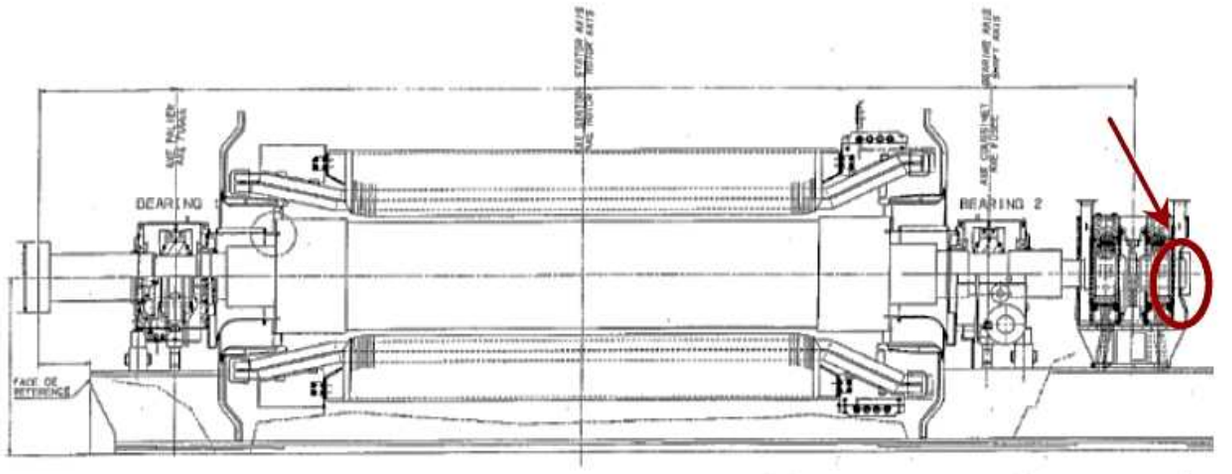

Figure 8. Chosen balancing plane of the generator shaft end; *Source:Gupta,etal* (2003)

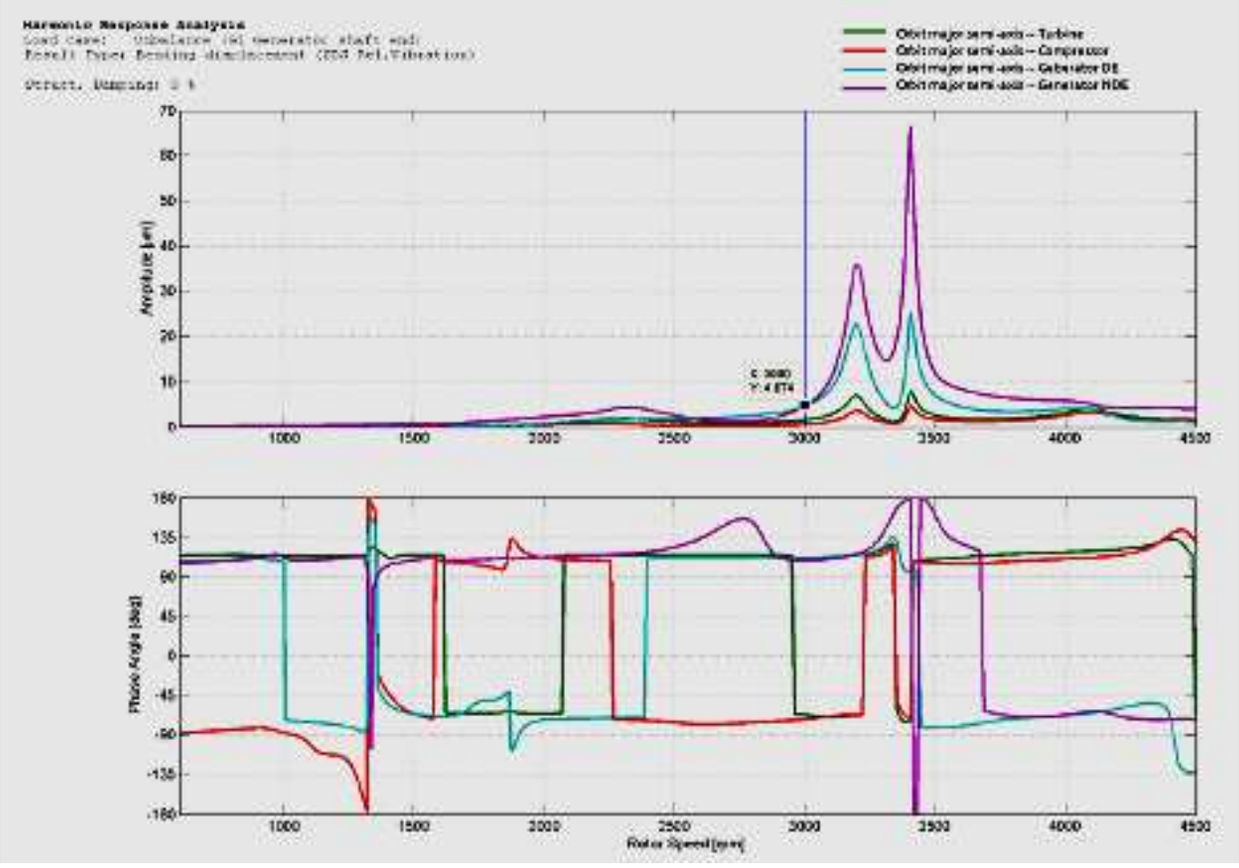

Figure 9. G1 unbalance of the shaft end; *Source:Gupta,etal.* (2003)

This unbalance response shows that there is a certain influence at 50Hz due to this added unbalance, however to balance the shaft end, a correction mass of about 15 times higher would be needed to bring down the actual shaft vibration amplitudes to acceptable levels. The resulting dynamic behaviour of the shaft line is shown in figure 10 and shows that there is an important reduction of the relative shaft vibrations around 3000rpm. This confirms of course that this shaft end mode was the main reason for the increased shaft vibrations.

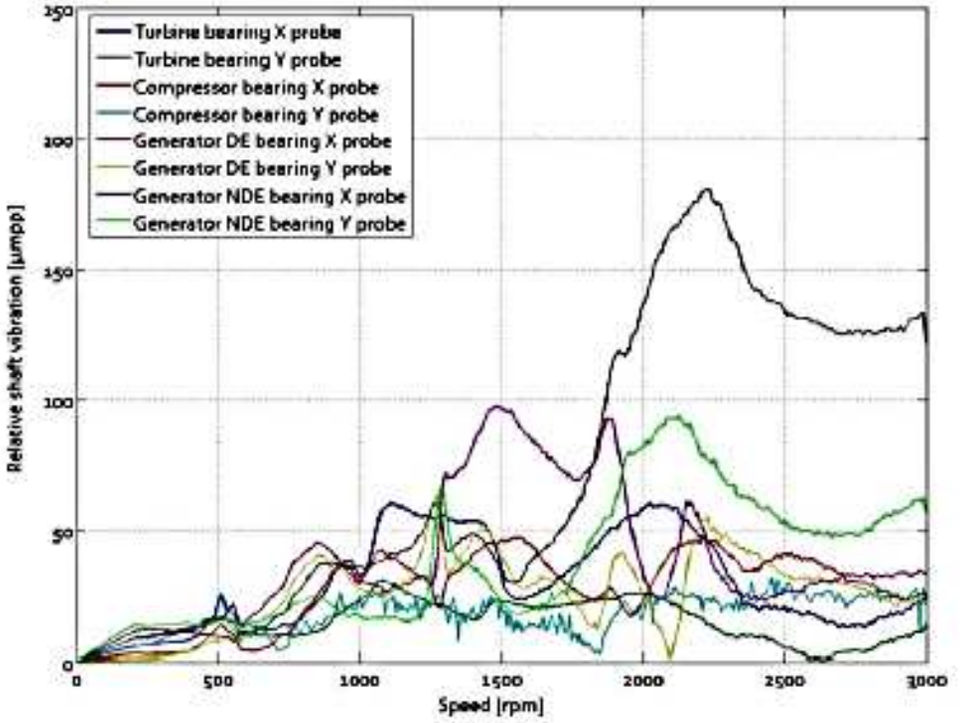

Figure 10. Relative shaft vibration amplitudes after balancing; *Source:Gupta,etal.* (2003)

This balancing correction was done completely remotely. Only a local maintenance responsible went on-site to attach the balancing weight. This made it possible to react quickly on this vibration issue and reduced the unforeseen downtime of the unit to a minimum. The unit could be restarted the same day without any vibrations alarms and a more extensive balancing of the present residual unbalance of the rotor could be scheduled at a more appropriate moment in the maintenance planning.

3. Methodology for blade vibration analysis

Rotor shafts are amongst rotor dynamic components subjected to perhaps the most arduous working condition in high performance rotating equipment used in process and utility plants such as high-speed compressor, steam and gas turbines generators, pumps, etc. Although usually quite robust and well designed, shafts in operation are sometimes susceptible to serious defects that develop without much warning.

In exploitation of rotating machines, some of the observed phenomena are considered to be particularly undesired from the view point of effectiveness and safety. Excessive stress concentrations and rubbing effects occurring between stator and rotors attached to flexible shafts subjected to lateral vibrations can be given as examples of such a detrimental behavior. The modern responsible and heavily affected rotating machines must assure possibly high level of reliability, durability and safety in operation. For these reasons, their design process should be performed very thoroughly in order to obtain relatively small magnitude of unavoidable dynamic excitation, e.g. due to residual unbalance, gas pressure force or electromagnetic force. While aiming at realistic modeling of rotor shaft systems, the actual stochastic nature of important model parameters should be taken into account. In the previous section, different references have been made to the problems of rotor shaft dynamic modeling. A lot of reasons were given as regards to the need to the modeling approach; however, all-inclusive approach must be employed to tame the problems. This involves the understanding of the theoretical model of a rotor shaft, assessment of rotor-shaft vibration due to uncertain residual unbalances and as well as the modeling dynamic response analysis. Therefore, all the modification discussed in this chapter only affects the GT rotor shaft system.

3.1. Theoretical model of a bowed rotor shaft

A typical rotor with a bowed unbalanced shaft is presented in Ogbonnaya (2004). All phase angles are measured with respect to a reference timing mark on the shaft. Suppose the shaft has a residual bow of ∂_r and a phase of ϕ_r, then the mass centre of the disk would be displaced by a distance, e_u from the shaft centre line. This results in a dynamic unbalance response as the shaft rotates.

Suppose the magnitude and phase angle of the combined electrical and mechanical run-out respectively, then the total observed response is:

$$\partial = \partial_r + \partial_s + \partial_o \tag{7}$$

Where:

∂r=bow vector

∂s=response to the mass unbalance vector and the bow vector

∂o=run-out vector

Assumptions:

a. No gyroscopic pull occur (since the disc always rotates in its own plane)

b. Shaft mass is considered negligible (compared to the rigid disc mass)

c. Both shaft and disc rotate with uniform angular velocity, ω

d. The supports are taken as rigid

The equation of motion for a simple rotor with imbalance and shaft bow has been used to obtain the steady state non-dimensionalised rotor response as a function of rotor speed as follows:

$$\bar{z} = \frac{\bar{\delta}_r e^{-i\varnothing r} + f^2 e^{-i\varnothing m}}{1 - f^2 + 2i\xi f} \tag{8}$$

Where:

ϕ_o=angle between the rotor run-out vector and the timing mark (equation 9)

ϕ_r=angle between the bow vector and the timing mark

ϕ_m=angle between the mass unbalance vector and the timing mark

ϕ= phase angle between the shaft centerline response vector and the timing mark (equation 9)

f= frequency ratio, $\omega / \omega_{cr} = \dfrac{\text{rotational speed}}{\text{rotor critical speed}}$

ξ =damping ratio, c / c_{cr}

∂_r =residual bow

C=shaft damping, Nm/rad

C_{cr} =critical speed (with low compensation C)

Consider a shaft with electrical and/or mechanical run-out. The run-out vector is also non-dimensionalized by an unbalance eccentricity given by:

$$\bar{\delta}_o = \frac{\delta_o}{e_u}$$

Where e_u=unbalance eccentricity vector (this run-out vector is constant and independent of the shaft rotational speed).

Using the principles of superposition, the constant response due to run-out may be added to equation 3 for steady state response to yield:

$$\bar{z} = \frac{\bar{\delta}_r e^{-i\varnothing r} + f^2 e^{-i\varnothing m}}{1 - f^2 + 2i\xi f} + \bar{\delta}_o e^{-i\varnothing o} \tag{9}$$

If $\gamma=\phi_r-\phi_m$, then equation 9 becomes:

$$\bar{z} = \alpha_r \bar{\delta}_r e^{-i\varnothing r} + \alpha_r e^{-i\varnothing m} + \alpha_r \delta_o e^{-i\varnothing o} \tag{10}$$

http://dx.doi.org/10.5772/58829

Where:

α_r= influence coefficient due to bow=$\frac{1}{(1-f^2 2\mathrm{i}\,\xi\, f)}$

α_m=influence coefficient due to mass unbalance=$\frac{f^2}{(1-f^2 2\mathrm{i}\xi\, f)}$

α_0=influence coefficient due to run-out=1

Separating $\bar{z}$ in equation 10 into real and imaginary components $(\bar{z} = {}_r + \mathrm{i}_{\mathrm{i}})$, yields

$$\bar{z}_{\mathrm{r}} = \frac{\left(\bar{\delta}_r, \cos\varphi, + f^2 \cos\varphi_m\right)\left(1\text{-}f^2\right) - 2\varsigma f\left(\bar{\delta}_r, \sin\varphi_{\mathrm{r}} + f^2 \sin\varphi_{\mathrm{m}}\right)}{\left(1\text{-}f^2\right)^2 + \left(2\varsigma f\right)^2} + \bar{\delta}_0 \cos\varphi_0 \tag{11}$$

$$\bar{z}_i = \frac{\left(\bar{\delta}_r, \sin\varphi, + f^2 \sin\varphi_m\right)\left(1\text{-}f^2\right) + 2\varsigma f\left(\bar{\delta}_r, \cos\varphi_{\mathrm{r}} + f^2 \cos\varphi_{\mathrm{m}}\right)}{\left(1\text{-}f^2\right)^2 + \left(2\varsigma f\right)^2} + \bar{\delta}_0 \sin\varphi_0 \tag{12}$$

Therefore, the shaft amplification factor and phase angle are respectively:

$$\mathrm{A} = \sqrt{\bar{z}_r} + \bar{z}_i^2 \tag{13}$$

and

$$\theta = \tan^{-1}\left[\bar{z}_i \big/ \bar{z}_r\right] \tag{14}$$

respectively

For the response of the bowed rotor at slow roll, substitute f=0 into equation 15 to get:

$$\bar{Z}_o = \bar{\delta}_r e^{-i\varnothing r} + \bar{\delta}_o e^{-i\varnothing m} \tag{15}$$

$$\therefore \qquad \bar{z}_r\big|_{\mathrm{o}} = \bar{\delta}\cos\phi_{\mathrm{r}} + \bar{\delta}\cos\phi_{\mathrm{o}} \tag{16}$$

$$\text{and} \qquad \bar{z}_i\big|_{\mathrm{o}} = \bar{\delta}\cos\phi_{\mathrm{r}} + \bar{\delta}\cos\phi_{\mathrm{o}} \tag{17}$$

Note: for the case of bowed shaft, the run-out compensator and subtractor compensate for shaft run-out, thereby presenting the response for the rotor as if it had only unbalance with no run-out. Therefore, equations 9 and 10 are the quantities the compensator subtracts from the total response of a bowed rotor at all other speeds. Let this quantity be designated by $\bar{z}_c$ for a bowed rotor compensated for electrical/mechanical run-out.

$$\therefore \qquad \bar{z}_c = \bar{z} - \bar{z}_0 = \frac{\delta_r e^{-i\varphi_r} + f^2 e^{-i\varphi_m}}{1 - f^2 + 2i\xi f} - \delta_r e^{-i\varphi_r} \tag{18}$$

Rearranging equation (18) and combing like terms yields:

$$\bar{Z}_c = \frac{(f^2 - 2i\xi f)\bar{\delta}_r e^{-i\varnothing m}}{1 - f^2 + 2i\xi f} \tag{19}$$

which can also be put as:

$$\bar{Z}_c = \alpha_{rc}\bar{\delta}_r e^{-i\varnothing r} + \alpha_m e^{-i\varnothing m} \tag{20}$$

Where α_{rc}=influence coefficient for compensated bow and given by:

$\alpha_{rc} = \dfrac{(f^2 - 2i\xi f)}{1 - f^2 + 2i\xi f}$ as $\alpha_{rc} \to \alpha_m$ for *large* f.

The response due to compensated bow and an equal unbalance eccentricity are equal.

3.2. Mathematical modeling of dynamic response of GT rotor shaft

When a system is subjected to force harmonic excitation, its vibration response takes place at the same frequency as that of the excitation. Common sources of harmonic excitation are: unbalance of the rotating shaft, forces produced by reciprocating machines, or the motion of the machine itself. These vibrations are undesirable to equipment whose operation may be distributed. Resonance is to be avoided in general, and to prevent large amplitudes, vibration isolators are often used.

3.2.1. Response of single degree of freedom system

According to Ogbonnaya (2004), a rotor shaft can be modeled using the single degree of freedom system shown in figure 11(a) and the free body diagram as presented in figure 11(b).

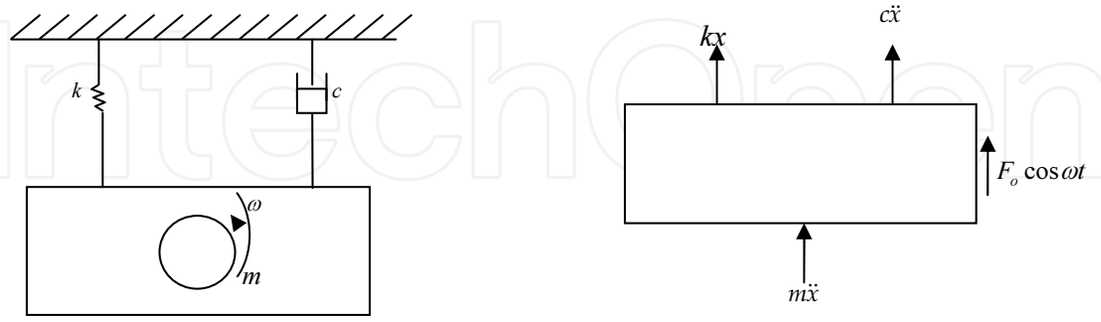

(a) Model of rotor shaft (b) Free body diagram

Figure 11. Model of a rotor shaft system

From the figures above, the equation of motion can be stated as shown in equation 21.

$$m\ddot{x} + c\dot{x} + kx = 0 \tag{21}$$

3.2.2. Impulse response approach

Figures 12 (a) and (b) show the forcing function in the form of a series of impulses and unit impulse excitation at t=ζ, while figure 12 (c) represents the impulse response function.

Here, consideration was given to the forcing function x(t) to be made up of a series of impulse of varying magnitude as shown in figure 12a. Let the impulse applied at time τ be denoted as $x(\tau)\,d\tau$. If $y(t)=H(t-\tau)$ denotes the response of the unit impulse excitation, δ (t-τ), it is called the impulse response function. The response to the total excitation is:

$$y(t)=\int_{-\infty}^{t} x(\tau)h(t-\tau)d\tau \tag{22}$$

Since h (t-τ)=0 when t < τ or τ > t, the upper limit of integration can be replaced by ∞ so that:

$$y(t)=\int_{-\infty}^{\infty} x(\tau)h(t-\tau)d\tau \tag{23}$$

By changing the variables from τ to θ=t – τ, equation 23 can be written as:

$$y(t)=\int_{-\infty}^{\infty} x(t-o)h(o)d\theta \tag{24}$$

The response of the system y(*t*) can be known if the impulse response function h (t) is known.

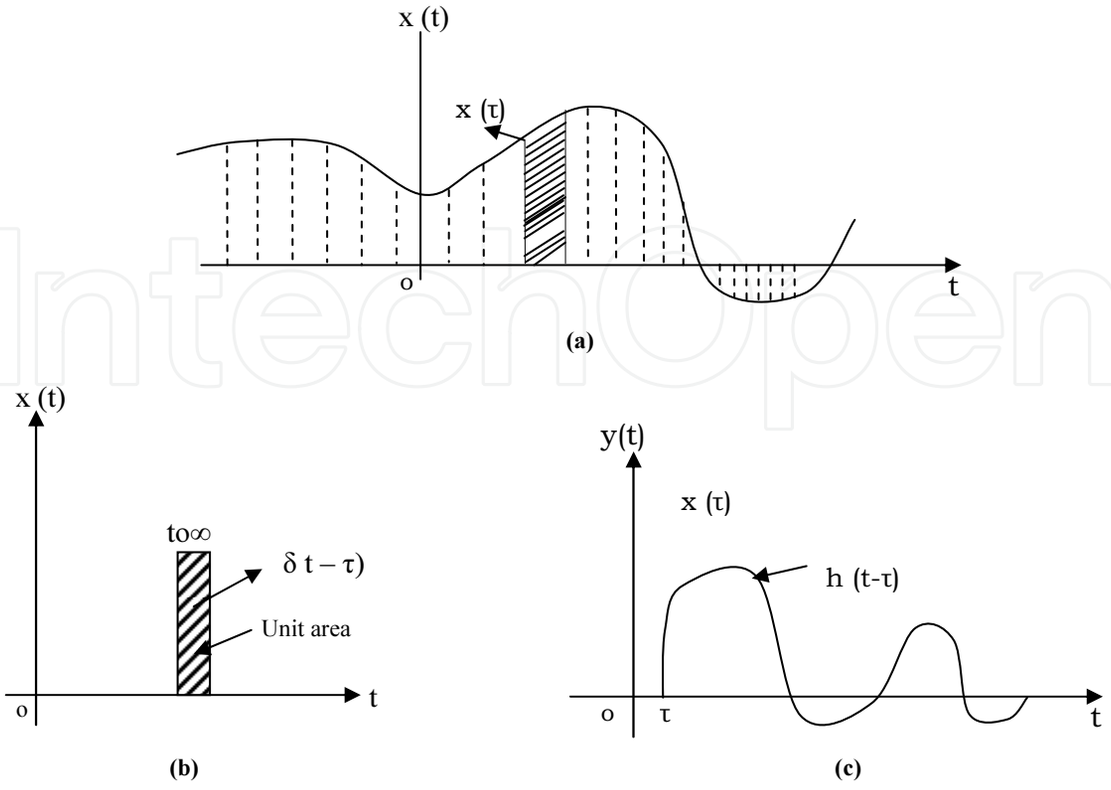

Figure 12. (a) forcing function in the form of series of impulses; (b) Unit impulse excitation at t=τ; (c) Impulse response function; *Source: Sadhu, (2006)*

3.2.3. Frequency response approach

In this case, the transient function x(t) can be expressed in terms of its Fourier transform x(ω) as:

$$x(t)=\frac{1}{2\pi}\int_{\omega=-\infty}^{\infty}x(\omega)e \tag{25}$$

Consider the forcing function of unit modulus as:

$$\bar{x}(t)=e^{i\omega t} \tag{26}$$

Its response can be denoted as;

$$\bar{y}(t)=H\left(_{\omega}\right)_{e}{}^{i\omega t} \tag{27}$$

Where: H (ω) is called the complex frequency response function. Thus, the total response is:

$$y(t)=H(\omega)x^{t}=\int_{-\infty}^{\infty}H(\omega)\frac{1}{2\pi}x\left(\omega\right)e^{i\omega t}d\omega \tag{28}$$

If y (ω) denotes the Fourier transform of the response function y (t), then:

$$y(t)=\frac{1}{2\pi}\int_{-\infty}^{\infty}x\left(\omega\right)e^{i\omega t}d\omega \tag{29}$$

Comparing equations 27 and 28 we get:

$$x(\omega)=H(\omega)x(\omega) \tag{30}$$

Equation (30) can be used to find the response of the system once H (ω) is known.

3.2.4. Computation of dynamic response of GT rotor shaft system

From the model of the rotor shaft system shown in figures 11(a) and (b), the equation of the motion for equilibrium can be written as:

$$\sum F=ma=m\ddot{x} \tag{31}$$

$F_o\cos\omega t+\omega-k(d_{st}+x)=m\ddot{x}$

Where d_{st} = elongation of the spring (meter)

$F_o\cos\omega t+\omega-kd_{st}-kx=m\ddot{x}$

But $\omega=kd_{st}$

$F_o\cos\omega t+kd_{st}-kd_{st}-kx=m\ddot{x}$

$F_o\cos\omega t-kx=m\ddot{x}$

$$m\ddot{x}+kx=F_o\cos\omega t \tag{32}$$

By considering damping force, equation (32) can be further expressed as:

$$m\ddot{x}+c\dot{x}+kx=F_o\cos\omega t \tag{33}$$

$$\ddot{x}+\frac{c}{m}\dot{x}+\frac{k}{m}x=\frac{\ddot{F}_o\cos\omega t}{m} \tag{34}$$

but $\frac{c}{m}=2\mu$ and $\frac{k}{m}=\omega_n{}^2$ (Ogbonnaya, et al; 2013); where μ is the slip factor which is the parameter describing how much the rotor exit flow angle deviate from the actual blade angle; i.e. fouling/corrosion factor. Hence, equation (34) is modified as:

$$\ddot{x}+2\mu\dot{x}+\omega_n{}^2x=0 \tag{35}$$

Equating the complementary function to zero, gives:

$$x_1=C_1e^{\left[-\mu+\sqrt{\mu^2-\omega^2}\right]t}+C_2e^{\left[-\mu+\sqrt{\mu^2-\omega^2}\right]t} \tag{36}$$

$x_1=C_1e^{\left[-\mu+\sqrt{\mu^2-\omega^2}\right]t}+C_2e^{\left[-\mu+\sqrt{\mu^2-\omega^2}\right]t}$

$x_2=[C_1+C_2t]e^{-\mu t}$

$x_3=e^{-\mu t}[A\cos\sqrt{(\omega^2-\mu^2)}t+B\sin\sqrt{(\omega^2-\mu^2)}t$

The general solution of equation (34) thus, is given by:

$$X=\frac{F_o}{m}\left[\frac{\sqrt{4\mu^2\omega^2+(\omega_n{}^2-\omega^2)^2}}{4\mu^2\omega^2+(\omega_n{}^2-\omega^2)^2}\cos(\omega t-\alpha)\right] \tag{37}$$

The overall solution is a combination of the complementary function and the general solution given as follows:

$$X=\frac{F_o}{m\sqrt{4\mu^2\omega^2+(\omega_n{}^2-\omega^2)^2}} \tag{38}$$

The vibration displacement amplitude is observed as:

$$F_o=XM\sqrt{4\mu^2\omega^2+(\omega_n{}^2-\omega^2)^2} \tag{39}$$

where:

$$F_o=XM\sqrt{4\mu^2\omega^2+(\omega_n{}^2-\omega^2)^2} \tag{40}$$

http://dx.doi.org/10.5772/58829

Figure 13 shows the flow chart for obtaining the dynamic response of a rotor shaft. This is actualized by evaluation of the program code written in C++programming language from figure 12a. The program helped in the calculation of dynamic response by inputting the values obtained from GT 17 of Afam Power Station into the equation 40. The result shows that the rotor vibration response takes place at the same frequency as that of the excitation.

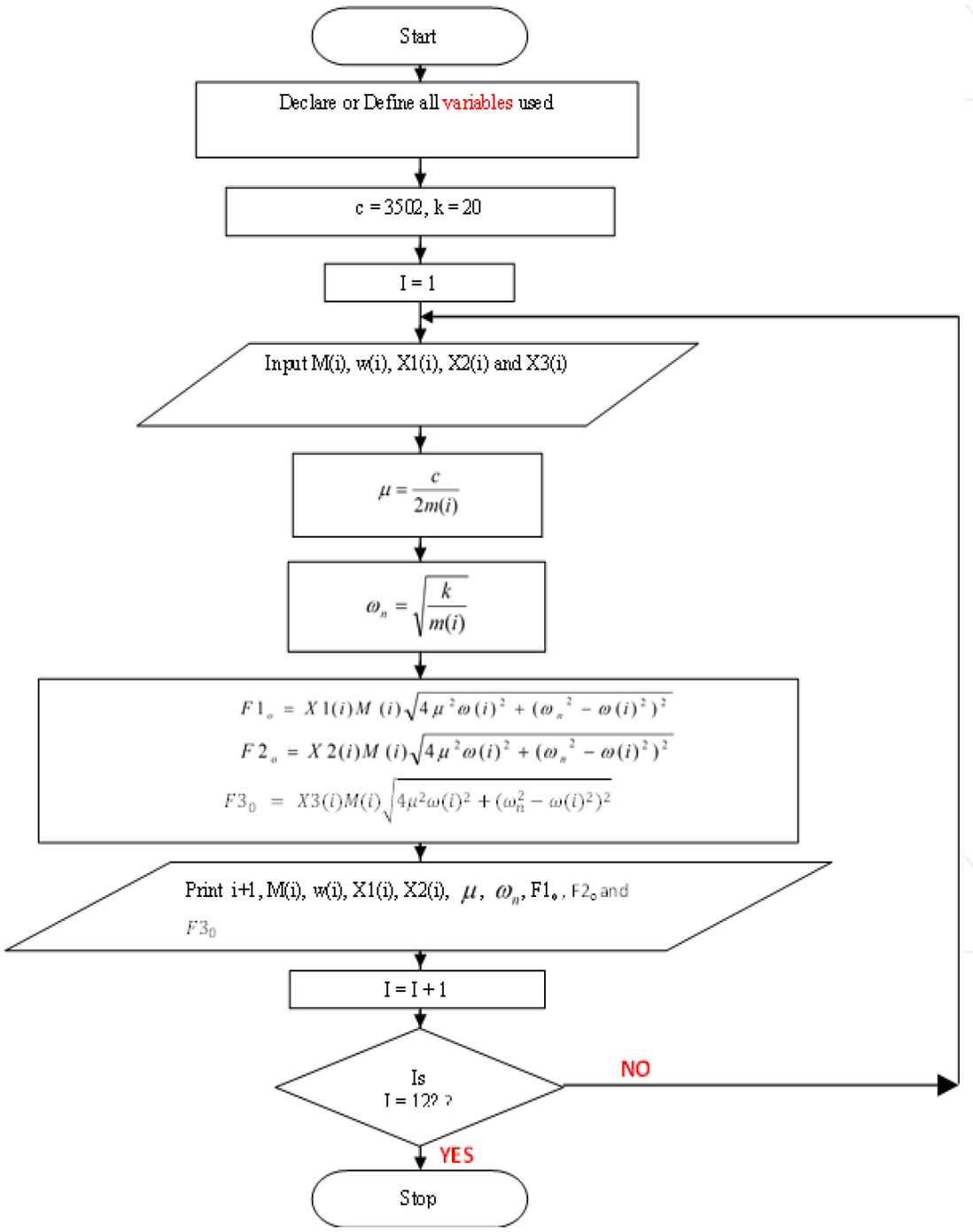

Figure 13. Program Flow Chart of the rotor Shaft Dynamic Response

4. Analysis

Gas Turbine, GT unit 17 is a healthy engine. The horizontal readings of natural frequency (ω_n) taken from healthy GT 17 and engine data are presented in Table 1, while the other parametric characteristics of the Afam GT 17 system used are shown in Appendix A. However, these readings were taken alongside the corresponding speed at different times for active and reactive loads.

Time (hr)	Speed (RPM)	Active load (KW)	Natural frequency, (ω_n)	Vibration amplitude (Br1) (mm)	Vibration amplitude (Br2) (mm)	Vibration amplitude (Br3) (mm)
01.00	3063	50	321.7	4.8	6.2	0.9
02.00	3076	50	322.3	4.8	6.2	0.8
03.00	3074	50	321.7	4.6	6.2	0.9
04.00	3077	50	322.3	4.9	6.2	0.8
05.00	356	50	320.4	4.9	6.2	0.9
06.00	3001	50	316.7	5.1	6.3	1.0
07.00	3063	45	321.0	5.1	6.5	1.0
08.00	3076	40	322.3	5.3	6.5	0.9
09.00	3028	40	318.6	5.0	6.7	1.2
10.00	3081	36	323.6	5.1	6.4	0.9
11.00	3053	35	319.8	5.2	6.5	1.0
12.00	3.53	45	316.0	5.2	6.4	1.2
13.00	3005	37	314.2	5.2	6.6	1.7
14.00	3060	42	319.8	5.0	6.7	0.9
15.00	3056	41	319.2	5.3	6.5	0.9
16.00	3021	41	319.2	5.1	6.6	0.9
17.00	3077	40	322.9	51.2	6.6	0.9
18.00	3070	42	318.6	5.0	6.5	0.9
19.00	3074	42	321.0	5.0	6.5	0.9
20.00	3074	47	322.9	5.0	6.4	1.0
21.00	3065	40	321.0	5.0	6.6	1.2
22.00	3072	42	421.7	5.0	6.5	1.4
23.00	3077	50	322.3	5.0	6.4	1.3
24.00	3086	30	321.7	5.0	6.3	1.2

Table 1. Operational Data from Healthy GT 17 of Afam Power Station

http://dx.doi.org/10.5772/58829

4.1. Discussion

Table 1 shows the result of vibration displacement amplitude of bearings 1, 2 and 3 as a function of time. From the graph presented in figure 14, it was observed that bearing 1 and 2 started vibrating as soon as the engine was powered, while bearings 3 delayed for some operational interval before vibrating. The graph shown in figure 14 also shows that the machine tends to vibrate in higher displacement amplitude and sometimes slows down as the engine continues in operation (i.e. in fluctuating manner).

Depicted in figure 15 is the graph of the response of the system against time. Here, it is shown clearly that the forcing function x (t) is made up of series of impulses of varying magnitude. The impulse response was found to correspond with the sinusoidal shape as expected.

Figure 16 conversely shows the graph of natural frequency against time. From the graph, the result shows that the natural frequency tends to vary with time. It is observed also that the vibration of the engine occurs as a function of natural frequency at a given time.

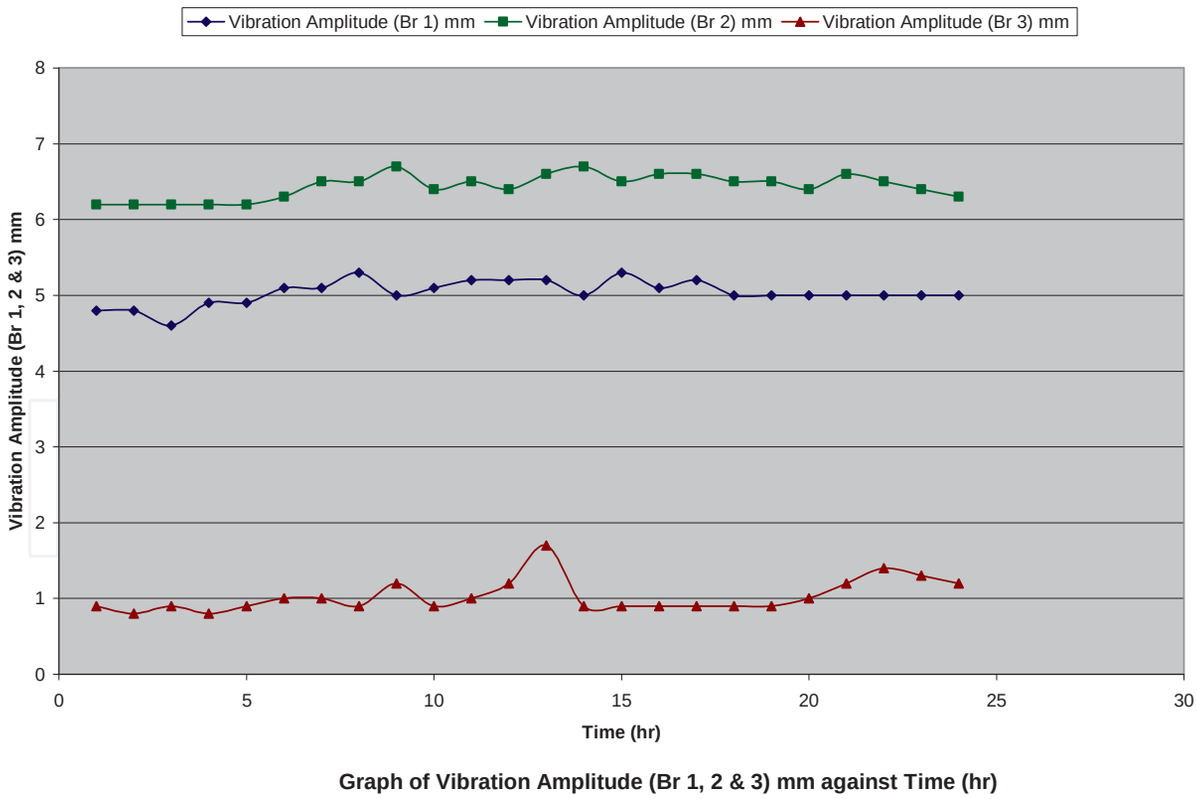

Figure 14. Vibration amplitude (Br 1, 2 & 3) mm against time (hr)

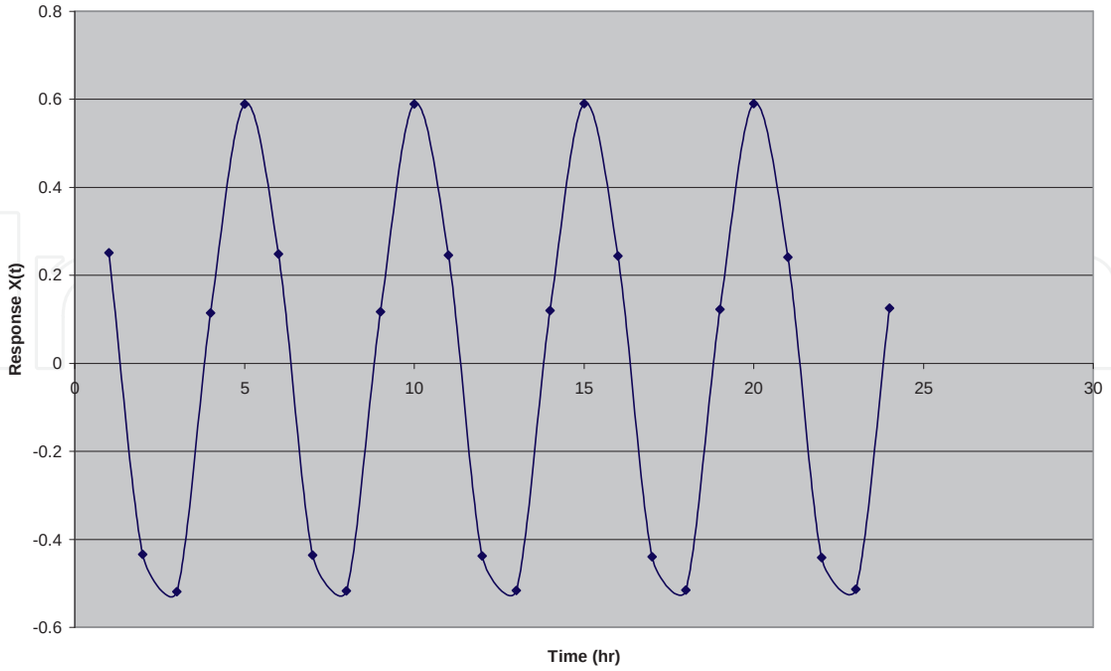

Figure 15. Response, X (t) against time (hr)

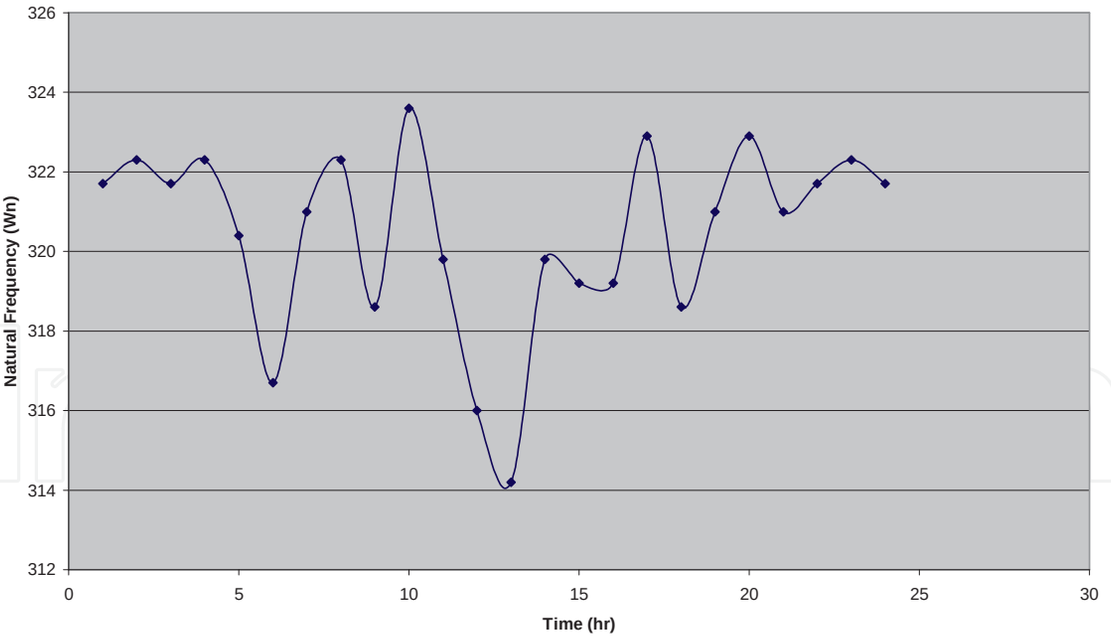

Figure 16. Natural frequency (ω_n) against time (hr)

Figure 17 further shows the graph of speed (rpm) with time. Hence, the sudden increase in speed as presented in the figure is capable of resulting to an increase in vibration at the given interval.

http://dx.doi.org/10.5772/58829

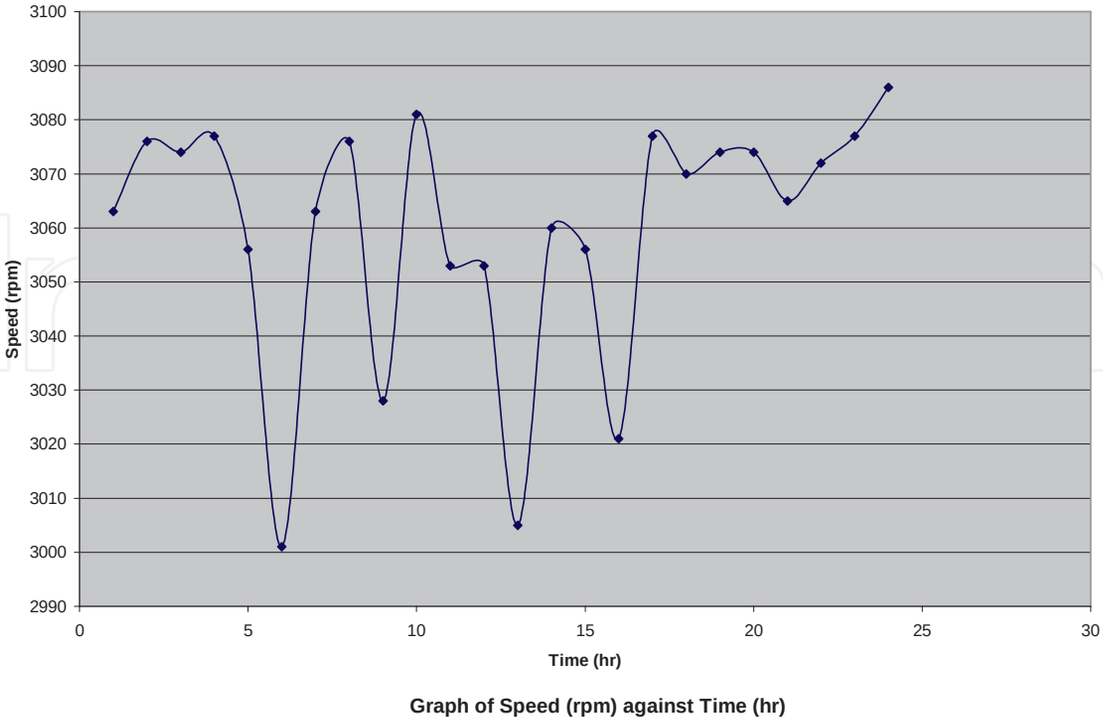

Figure 17. Speed (rpm) against time (hrs)

5. Conclusion

A work has been carried out on the modeling of dynamic response of marine GT rotor shaft systems. It is shown that when a system is subjected to force harmonic excitation, its vibration response takes place at the same frequency as that of the excitation.

To determine the response of the shaft under vibration, readings were collected from bearings 1, 2, and 3 of GT 17 in Afam thermal Station as shown in table 1, while the engine characteristics are shown in Appendix A. Equation 40 was developed to determine the response of the system under vibration. This mathematical equation is used to run a computer programme with a code in C++programming language.

6. Recommendations

The recommendations are as follows:

1. More attention should be paid to shaft vibrations as is the case with vibration on bearing.
2. Some factors which affect the performance of gas turbines on industrial duty should be considered while carrying out vibration based simulation of GT rotor shafts.

3. Errors and extraneous environmental factors should be put into consideration when modeling the response of rotor shaft under vibration.

4. GT rotor shaft systems should be provided with more supports to prevent adverse effects of eccentricity which leads to bow and whirl.

7. Appendix A

7.1. Characteristics of AFAM GT 17 system relevant to this work

Name of Equipment: Brown Boveri	Sulzer Turbo Maschinen
Manufacturer:	Asea Brown Boveri
Capacity:	75 MW
Year of Manufacture:	1981
Year of installation	1982
Year of commissioning	Nov 1982
Type:	13D
No of Turbine Rows:	5
No. of Compressor Rows:	17

Particulars of Rotor

Length of Rotor shaft:	8000mm
Moment of Inertia, I:	$586.2m^4$
Modulus of Elasticity, E:	$207GN/m^2$
Mean Diameter, :	1400mm
Density, ρ:	$7850kg/m^3$
Modulus of Rigidity, G:	$80GN/m^2$
Mass of Turbine shaft:	23500kg
Mass of Compressor shaft:	24000kg
Natural frequency, ω_n:	350rad/s
Damping Ratio, ζ:	0.9
Spring stiffness, K:	$1.5x10^6N/mm$
Maximum vibration limit:	7.0mm/s

Author details

E.A. Ogbonnaya[1], R. Poku[1], H.U. Ugwu[2], K.T. Johnson[3], J.C. Orji[3] and N. Samson[3]

1 Department of Marine/Mechanical Engineering, Niger Delta University, Wilberforce Island, Bayelsa State, Nigeria

2 Department of Mechanical Engineering, Michael Okpara University of Agriculture, Umudike, Abia State, Nigeria

3 Department of Marine Engineering, Rivers State University of Science and Technology, Port Harcourt, Rivers State, Nigeria

References

[1] Api 617 (2002) Axial and centrifugal compressor and expander-compressor for petroleum, chemical and gas industry services, 7th edition, Washington D.C, API publishing.

[2] Bader K.A (2010) Rotor dynamic analysis requirements in API Standards with case studies.Proceedings of *ASME Turbo Expo*. 2010. Power for land and sea and air, June 14-181010 Glasgow Paper No. GT 2010-23127.

[3] Choi, S.Y. and Mau (2009) Dynamitic analysis of geared rotor-bearing systems by the transfer matrix method.*ASME Design Engineering Technical Conferences*.(Part B), 84: 2967-2976.

[4] Eshleman, R. and Eubanks, A (2007) On the critical speeds of a continuous rotor, *Journal of Engineering for Industry*, 91: 1180-1188.

[5] Gupta, K. D.,Gupta K.and Athre, K (2003) Unbalance response of a dual rotor system: (theory and experiment) *Trans. Journal of Vibration and Acoustics*, 115: 427-435.

[6] Harilirua and Srinivasan P.S. (2010). Vibration analysis of flexible coupling by considering unbalance, *Middle East Journal of Scientific Research* 5 (5): pp 336-345, 2010.

[7] Hibner (2007) Dynamic response of viscous-damped multi-shaft jet engines. *Journal of Aircraft*, 12(4): 305-312.

[8] Iwatsubo, S.Arii, and Kawai, R, 2009. Coupled lateral-torsional vibration of rotor system trained by gears, *Bulletin of ASME*, 27(224): 271-277.

[9] Kahraman, A., Ozguven, H. N.,Houser D. R.and Zakrajsek, J. J, 2009.Dynamic analysis of geared rotors by finite elements, Transactions.*Journal of Mechanical Design*, 114: 507-514.

[10] Kris, M., Marco, P and Koenraad De B, (2010) Rotor dynamic modeling as a powerful support tool for vibration analysi on large turbomachinery.*The 8thIFFoMM International Conference on rotor dynamics,* September 12-15, 2010/kist, seoulkora, pp 700-706.

[11] Lee, W. and Ha, D.H. (2003) Coupled lateral and torsional vibration characteristics of a speed increasing geared rotor-bearing system, *Journal of Sound and Vibration*, 263(4): 725-742.

[12] Lida., Tamura K and Kikuch, H (2009) Coupled torsional-flexural vibration of a shaft in a geared system of rotors (1st report), *Bulletin of the ASME*, 23(186): 2111-2117.

[13] Mitchell, L.D. and Melleu, D.M. (2005) Torsional- lateral coupling in a geared high-speed rotor system, *ASME Design Engineering Technical Conferences*. 3 (Part B), 84(2): 977-989.

[14] R. B., Bhat,T. S and Sankar (2009) Coupled torsional flexural vibration of a geared shaft system using finite element method, *Shock and Vibration Bulletin* (Part 3), 55: 13-25.

[15] Ogbonnaya, E.A. (2004) *Modeling vibration base faults in Rotor Shaft of Gas Turbine*. Ph.D work Department of Marine Engineering, Rivers State University of Science and Technology, Port Harcourt, Rivers State, Nigeria, pp 64- 79.

[16] Ogbonnaya, E.A., Johnson, K.T, Ugwu, H.U and Orji, C.U (2010) Component model-based condition monitoring of a Gas Turbine, *ARPN Journal of Engineering and Applied Sciences*, ISSN 1819-6680, Vol., No. 3, p 40

[17] Ogbonnaya, E.A., Ugwu, H. U. and Diema, E.J (2013) A model-based mixed data approach for optimizing the performance of an offshore gas turbine compressor, Journal of Vibration Analysis, Measurement and Control, *Columbia International Publishing,* doi:10.7726/jvwp.2013.1001, pp30-43

[18] Rao, J.S., Chang, J. R and Shiau, T. N2007. Coupled bending-torsion vibration of geared rotors, *ASME* Design Engineering Technical Conferences. 3 (Part B), 84-2: 977-989.

[19] Rao, J.S, (2006) *Rotor Dynamics*, 3rd edition, New Age International Publishers, India.

[20] Shiyu, Z. and Jianjun S. (2001) Active balancing and vibration control of rotating machine: *A survey journal of shock and vibration digest*. vol. 33, No. 4 July, 2001. Pp 361-371 (C) September, 2001 Saye Publication.

[21] Surial, A and Kaushal A. (2008) Dynamic analysis of flexible turbo-rotor system using super elements.Rolls Roycc, Materials Polytechnics University Toronto Canada, pp 1-8.

[22] Zhu, X, and Andres, S.L., (2007).Rotor dynamic performance of flexure pivot hydrostatic Gas bearing for oil free turbo machinery *ASME . Eng. Gas Turbines Power*, 129 pp 1020-1027.